Environmental Modelling and Software 143 (2021) 105097

Contents lists available at ScienceDirect

Environmental Modelling and Software

journal homepage: www.elsevier.com/locate/envsoft

Streamlined wildland-urban interface fire tracing (SWUIFT): Modeling wildfire spread in communities

Nima Masoudvaziri *, Fernando Szasdi Bardales, Oguz Kaan Keskin, Amir Sarreshtehdari, Kang Sun, Negar Elhami-Khorasani

University at Buffalo, Buffalo, NY, USA

ARTICLE INFO

Keywords:
Wildfires
Wildland-urban interface
Community
Fire spread
Modeling

ABSTRACT

The wildland-urban interface (WUI) is defined as a geographic area where human developments and flammable vegetation merge in a wildfire-prone environment. Losses due to wildfire have been rising in the past decade, attributed to changes in vegetation growth, fuel availability, and increased land developments in WUI. This paper studies the process of wildfire spread inside WUI communities. The fire spread rate within WUI communities is determined for nine wildfires that were ranked among the most destructive wildfires in North America. An improved quasi-empirical model that considers radiation and fire spotting as modes of fire spread inside a community is proposed. The new model is validated using the documented spread rates during the 2007 Witch and Guejito fires and the 2017 Tubbs fire. The proposed model is computationally efficient and can be used to quantify fire spread rate and the number of affected structures inside a community during a wildfire event.

1. Introduction

Wildfires have always been part of the natural landscape for a healthy ecosystem, yet these fires are projected to become more frequent and intense due to changing weather patterns and human suppression activities in the past century. The economic and social impacts of wildfires have been rising in recent years and now represent a global concern. As of November 2020, 6 out of the 10 most destructive wildfires in the US, in terms of insured losses, happened in 2017 and 2018; also 13 out of the 20 most destructive fires, in terms of structure losses, happened since 2017 (Insurance Information Institute, 2020; California Department of Forestry and Fire Protection, 2020). Direct and indirect consequences of wildfires, including utility disruptions and environmental impacts have been significant (Masoudvaziri et al., 2020). The current approach in managing the fire hazard within communities is neither sufficient nor sustainable. Over the past several decades, fire safety research has spent a great deal of effort to understand fire dynamics inside buildings. In parallel, significant research has been conducted to understand wildfire behavior in the wildland area (Cruz et al., 2018; Bakhshaii and Johnson, 2019). But research on large outdoor fires within communities (e.g., due to wildfires), and development of codes and standards for such fires lag behind. A workshop by the American Society for Testing and Materials (ASTM) concludes that current codes and standards for communities susceptible to wildfire risk are not adequate (Manzello and Quarles, 2015).

The wildland-urban interface (WUI) is defined as a geographic area where human developments and flammable vegetation merge in a wildfire-prone environment (International Code Council, 2018). Not all the WUI communities are threatened by wildfires as several conditions, such as the risk of extreme fire events and the lack of protection and defense for buildings inside WUI communities, should occur concurrently (Cohen, 2008; Stein et al., 2013; Caton et al., 2017). In this paper, any mention of communities or WUI communities refers to the WUI communities that are affected (attacked) by wildfires.

Although extreme fire hazards cannot be eliminated, the amount of incurred damage depends on decisions made by policymakers and engineers and the attitude towards risk. The US Departments of Agriculture (USDA) and Interior (DOI) developed the National Fire Plan (USDA and DOI, 2007) after the devastating destruction of communities due to wildfires in 2000. In 2001, a 10-year Comprehensive Strategy Plan was developed to reduce wildfire risks to communities and the environment (USDA and DOI, 2007). This effort led to the Healthy Forests Restoration

* Corresponding author. Department of Civil, Structural and Environmental Engineering, University at Buffalo, NY, USA.
E-mail addresses: nimamaso@buffalo.edu (N. Masoudvaziri), fszasdib@buffalo.edu (F. Szasdi Bardales), okeskin@buffalo.edu (O.K. Keskin), amirsarr@buffalo.edu (A. Sarreshtehdari), kangsun@buffalo.edu (K. Sun), negarkho@buffalo.edu (N. Elhami-Khorasani).

https://doi.org/10.1016/j.envsoft.2021.105097
Accepted 20 May 2021
Available online 31 May 2021
1364-8152/© 2021 Elsevier Ltd. All rights reserved.

Act of 2003, which developed a framework for Community Wildfire Protection Plans (CWPPs) that calls for "communities to work collaboratively to develop CWPPs; the plan must identify and prioritize fuel treatment and set forth strategies to reduce the ignitability of houses and other infrastructure" (USHF, 2006). In May 2016, the White House (2016) issued an executive order to "mitigate wildfire risks to Federal buildings located in the WUI, reduce risks to people, and help minimize property loss due to wildfire." As a result of these efforts, a number of programs (such as Firewise (NFPA, 2021)) have been developed to provide guidance to communities for wildfire mitigation actions. Yet, the federal programs have focused more on wildland fire management (e.g., prescribed fires) and not sufficiently addressed the equally important community aspects. This is affirmed by the increasing WUI losses in recent years, while the impacts of fire on communities, lives, and properties can be managed by better understanding the problem and establishing proper policies.

Mathematical models are needed to investigate the process of fire spread in a WUI community. In a WUI community, a fire line advances based on three primary mechanisms: thermal radiation, direct flame contact, and firebrands. A comprehensive model would integrate these three mechanisms of fire spread, but such a validated model for application to WUI communities does not exist yet. Empirical fire spread models have been developed for the problem of fire following earthquake, but they have not been validated for WUI communities under wildfires. Many of the existing fire spread models are semi-empirical (Lee et al., 2008; Mahmoud and Chulahwat, 2020) with a few coarse attempts to include physics-based processes such as spotting and thermal radiation (Mahmoud and Chulahwat, 2018; Li and Davidson, 2013a, 2013b; Himoto and Tanaka, 2008; Iwami et al., 2004; Lee and Davidson, 2010a, 2010b; Nussle et al., 2004; Otake et al., 2003). The majority of urban fire spread models are developed in Japan for post-earthquake fire spread and are suitable for an urban environment involving equally spaced and equally-sized square buildings in dense urban areas (Hamada, 1975; Himoto et al., 2008). Lee and Davidson (2010b) have developed a more comprehensive spread model for post-earthquake fires. The spread model considers fire evolution within a room, from room to room inside a building, and from building to building by flame spread, but the level of required input information implies a number of assumptions hindering practicality for application to a community.

This paper starts with assessing the suitability of an existing urban fire spread model to predict fire progression inside a WUI community. Fire spread rate within communities is determined for nine wildfires, ranked among the most destructive wildfires in North America. The same nine fires are analyzed using a simplified approach to assess the validity of an existing model. In addition, the paper proposes a quasi-empirical model, as categorized per Sullivan's review (Sullivan, 2009), which considers radiation and firebrand mechanisms as modes of fire spread inside a community. The proposed model is validated using the documented spread rates during the 2007 Witch and Guejito fires and the 2017 Tubbs fire. The two selected communities as part of the validation study have different characteristics in terms of layout and building density, wind velocity during the wildfire event, etc., demonstrating the applicability of the model to capture different scenarios.

2. Fire spread rate during recent fires in WUI communities

Fire Spread Rate (FSR) inside a WUI community refers to how fast the fire travels inside that community. The FSR in this study is calculated as the distance between coordinates of two locations in the community, where fire spread occurred, divided by the corresponding time duration for which the fire traveled between the two coordinates. The value of FSR can vary during a fire event due to heterogeneity in land cover, topography, and wind patterns; therefore, the mean value should be taken to characterize the event within a community. A fast-approaching fire from the wildland reduces the available time for evacuation and for first respondents to control the fire propagation. When ignitions occur faster than the number of structural fires that are being put out by the fire crews, a conflagration can occur within a neighborhood and the fire becomes out of control.

Table 1
Fire spread rate (FSR) within communities, reported as meters/hr, for recent fire events in North America.

Fire/Date	Observed FSR (m h^{-1})
1. Tunnel Fire, 1991	200
2. Cedar Fire, 2003	932
3. Witch and Guejito Fires, 2007	340
4. Bastrop C. C. Fire, 2011	612
5. Horse River Fire, 2016	1385
6. Tubbs Fire, 2017	1780
7. Thomas Fire, 2017	528
8. Camp Fire, 2018	1535
9. Woolsey Fire, 2018	771

Table 2
Application of the Hamada model to calculate fire spread rate (FSR) within communities, reported as meters/hr, for recent fire events in North America.

Fire/Date	Average wind speed (m s^{-1})	Built-upness	FSR prediction - Hamada model (m h^{-1})
1. Tunnel Fire, 1991	7.6	0.33	271
2. Cedar Fire, 2003	3.6	0.10	238
3. Witch and Guejito Fires, 2007	10.3	0.11	977
4. Bastrop C. C. Fire, 2011	5.8	0.04	415
5. Horse River Fire, 2016	5.8	0.31	293
6. Tubbs Fire, 2017	5.8	0.15	358
7. Thomas Fire, 2017	8.0	0.24	514
8. Camp Fire, 2018	7.2	0.10	522
9. Woolsey Fire, 2018	4.9	0.29	262

Fire spread data within the wildland is available for most of the historic wildfire events and is often represented as increments in the burned area over a specific period of time (usually in the range of several hours). Fire contours, published by agencies, including but not limited to the California Department of Forestry and Fire Protection (CAL FIRE), the United States Geological Survey (USGS), and the U.S. Forest Service, show the borders of regions that have been burned by a fire at a certain point in time during the fire event. The precision of this information and satellite images are usually adequate to describe and study the fire in the wildland, but that is not the case for most of the fires inside a community due to the much higher spatial and temporal resolution required. Despite its importance, the FSR inside communities affected by wildfires is not always reported, and in many cases, precise information to determine the FSR is not available.

The required information on fire propagation and characteristics of communities to calculate FSR can be obtained from different sources such as reconnaissance reports, satellite images, aerial images from unmanned aircraft systems, and social media. Satellite images are reliable sources of information; however, current satellite images do not offer an ideal temporal resolution for tracking the advancement of fire inside a community. In most cases, two different satellite images of the same fire event are separated by a gap of several hours, which allows for monitoring fire spread on the wildland but do not capture the evolution of an event within a WUI community. It should also be noted that the current spatial resolution of freely available satellite images is approximately one pixel for every 10–60 m (GISGeography, 2021). Considering the size of typical WUI structures (with an average length between 16 and 25 m), some information could be lost if satellite images with lower resolution were used.

Based on the above, satellite images were used to quantify the FSR in

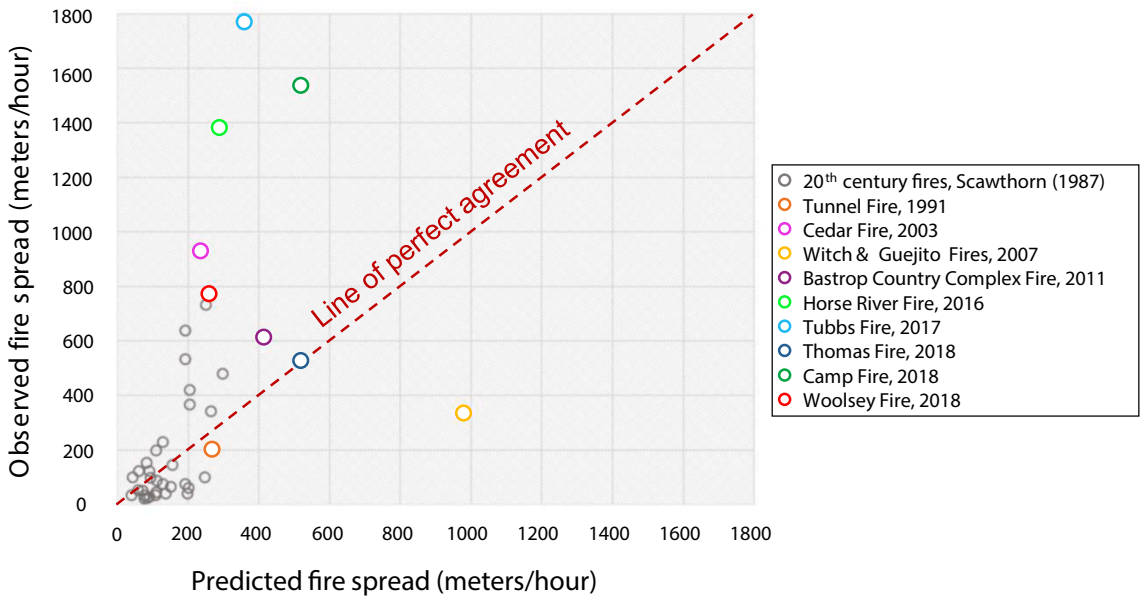

Fig. 1. Comparison of observed FSRs with predictions of the Hamada model for historic and recent fires.

WUI communities for nine of the most damaging recent fire events in the US, as listed in Table 1 (details of data sources for the nine events are provided in Szasdi Bardales (2019) and the associated wind speeds are provided in Table 2). Meanwhile, Scawthorn (1987) provides a list of historic 20th century North American urban fire events for which data were available to calculate the FSR. This list includes events as old as the 1900 Ottawa and Hull fires in Canada to a fire event in 1985 in Philadelphia, PA.

3. Existing simplified fire spread models

Simplified models are usually developed using empirical approaches and by performing regression analysis of data from past events. Such an approach was used as the first attempt in modeling inter-building fire spread for urban scenarios, dating back to the middle of the 20th century. One of the characteristics of simplified models is that they are straightforward to implement, without the need for complex computational platforms. The empirical equations in these models relate the FSR with the parameters that are known to influence fire propagation. The precision in these models is directly related to the reliability of the input data and the number of time steps used for the analysis. In general, the existing simplified fire spread models for application in community fires were generated specifically for the case of post-earthquake fires. The two most commonly used simplified models are the Hamada Model (Hamada, 1975) and the TOSHO Model (Tokyo Fire Department, 1997). This paper will focus on the Hamada model, while more information on the TOSHO model can be found in Tokyo Fire Department (1997). It should be noted that the HAZUS program developed by Federal Emergency Management Agency also implemented the same version of the Hamada model to assess the risk of fire spread after an earthquake in a community (Scawthorn, 2009; FEMA: HAZUS, 2014).

The Hamada model characterizes fire spread as a function of wind velocity and the average distances between buildings in a community (Hamada, 1975). The FSR coefficients are determined based on empirical relationships from past Japanese urban fire events, including the fire after the 1923 Kanto Earthquake, and wartime fires (Scawthorn, 2005). The model assumes an elliptical shape for the fire expansion, and the spread is faster in the downwind direction (aligns with the major axis of the ellipse), and slower in both the sidewind and upwind directions. The model simplifies the locations of the structures in a regular grid. All the structures are considered to have the same construction material and dimensions. The model does not consider the streets as fire barriers, and therefore street layouts are not included as an input. As an input, the model requires the user to provide information on the average length of one side of the buildings, the average distance between buildings, the wind velocity, and the average building density ratio within the community, represented by the built-upness factor. For brevity, the series of equations are not provided here and can be found in Szasdi Bardales (2019).

The Hamada model was applied to the nine recent fire cases discussed in Section 2. Detailed data, such as building layout in the community and wind speed during the fire event, was collected to simulate the fire events. The predicted FSR based on the Hamada model is listed in Table 2. A similar exercise was performed by Scawthorn in 1987 (Scawthorn, 1987). The Hamada model's predicted FSR for 32 historical 20th century cases was also collected and included in this study. Fig. 1 shows the comparison of the observed versus predicted FSR values for the nine investigated fire events (in color) as well as older 20th century fires (in gray). Scawthorn (1987) concluded that the Hamada model predictions agreed well with most of the observed FSRs, except for a group of cases in which fire spread by firebrands between wooden buildings was significant. Meanwhile, it is clear that, in the majority of recent fires (six out of nine wildfire events), the model underestimates the fire spread rate within the communities and is not able to capture the true behavior (See Table 1 and Fig. 1). Most of these recent fires in the US and the Canadian communities correspond to WUI wildfires at times of high winds and dry weather, conditions that significantly differ from those on which Hamada's model is based on. The Horse River Fire (2016), Tubbs Fire (2017), and Camp Fire (2018) especially accentuate the level of such underestimation with an average error of 320%. These results show a necessity for developing a new model that is capable of replicating the characteristics of modern WUI fires.

4. The proposed streamlined wildland-urban interface fire tracing (SWUIFT) model

This section proposes a new quasi-empirical model to simulate fire propagation in WUI communities; the proposed model is validated against observed data. The primary mechanisms of fire spread between buildings are thermal radiation, fire spotting by firebrands, and direct

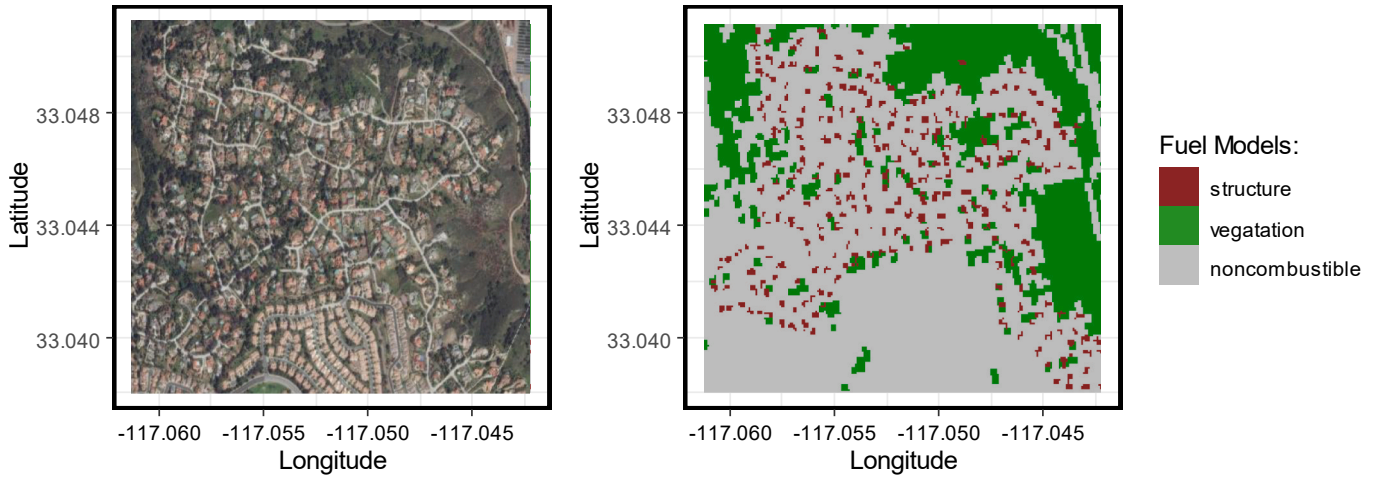

Fig. 2. Application of the fuel model to the Trails community in California and its corresponding input raster for the SWUIFT model.

flame contact. The current version of the proposed model incorporates thermal radiation and firebrands, while future work will expand on the model to include direct flame contact. An efficient fire spread model should balance between fidelity, the availability of input data, and fast execution. The proposed model has been developed to apply physics-based principles, while maintaining some of the advantages of simplified models, to have an efficient implementation and to reduce the computational cost.

The proposed model simplifies the community layout into a regular grid of cells. The content of each cell can take one of the three predefined fuel models: structure, vegetation, and non-combustible. The model captures the dynamic nature of a fire event by predicting the status of the fire within the community at individual time steps of 5 min. The model records the thermal radiative flux and the firebrands that have landed at any cell for every time-step and determines the status of individual structures and the duration of a fire in a specific structure. It also accounts for variable wind speed at every time step. The following sections provide details of the model mechanics, implemented fire spread modes, and the corresponding assumptions in the model.

4.1. Layout and wind

The proposed SWUIFT model characterizes fire events by two features: (1) community layout, and (2) wind speed and direction. A given community layout is rasterized into 10 × 10 m grids. The selected spatial resolution of 10 m captures a reasonable level of granularity while keeping the computational cost manageable. Here, three fuel models are introduced: structure, vegetation, non-combustible. The fuel model is a parametrization of different properties of the fuel bed and facilitates fuel bed classifications to be used as an input to the spread model (Scott, 2005). Each grid cell is assigned a fuel type based on the dominant (larger than 50%) land cover in that cell. For this purpose, the LANDFIRE's 13 Anderson Fire Behavior Fuel Model (Anderson, 1981; Reeves et al., 2009; Rollins, 2009) and Microsoft's Building Footprints (Microsoft, 2019) are retrieved and processed. Vegetation is defined as any vegetation with a height greater than 1 ft. The non-combustible classification represents land covers such as parking lots, roads, water bodies, etc. Fig. 2 demonstrates the application of the defined fuel model to the Trails community in California (to be discussed in detail in Section 5).

Wind data is the other input for the model, which should be provided for every time step. Forecast data can be used for predicting scenarios and planning applications, while historic data from the closest weather station to a community can be used to replicate an event. The model requires average wind speed and 3-s wind gust as inputs, where the wind speed is randomly selected for each time step assuming 80% likelihood for average wind speed and 20% likelihood for the wind gust.

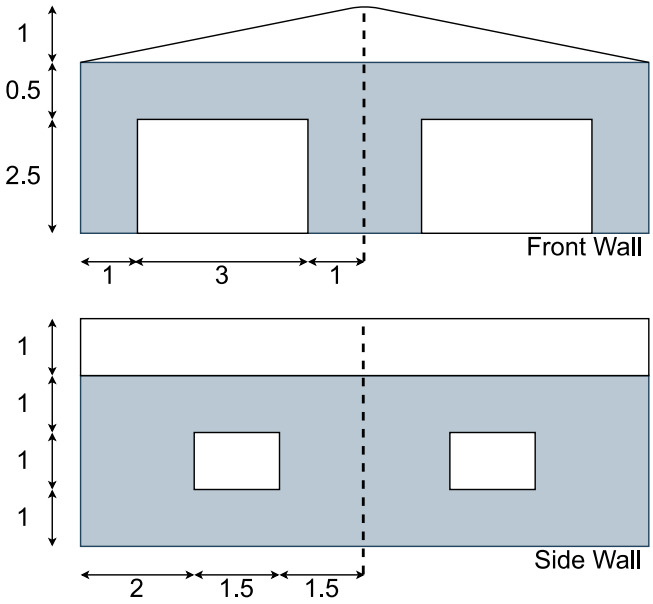

Fig. 3. Typical fire compartment configuration in a structure cell, dimensions are in meters.

4.2. Mechanics of the model

The SWUIFT model simulates the fire spread, and similar to other spread models requires the initial ignition(s) (grid cell location and time step) as an input. Ignitions can be defined both outside the community (i.e., an approaching fire line from the wildland) and inside the community (i.e., where firebrands cause ignition ahead of the wildfire perimeter reaching the community). The model is capable of accounting for any number of ignitions over the duration of the simulation. Once an ignition is defined, the model tracks the fire development. A structure cell can be ignited by either radiative heat or firebrands, and when the fire is at the fully developed phase, the cell emits energy and generates firebrands. A vegetation cell can only be ignited by firebrands, and when burning, it generates firebrands. Noncombustible cells do not ignite and have no positive contribution to the fire spread.

All structures in the WUI community are assumed to be residential housings. Each structure cell is coded to behave as a burning compartment of 10 × 10 m with the configuration illustrated in Fig. 3. The

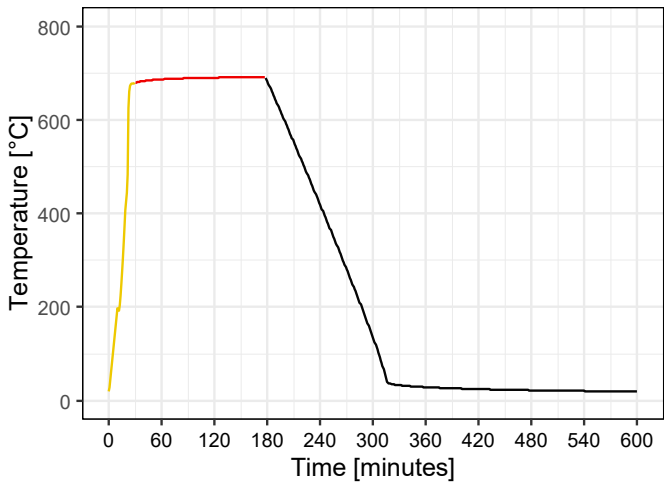

Fig. 4. Analysis for compartment fire. An ignited structure cell experiences three stages over time: developing (yellow), fully-developed (red), cooling/burnt (black).

compartment boundaries are assumed to be 10-cm thick normal wood. The typical temperature-time evolution for the assumed configuration is generated using OZone (Cadorin and Franssen, 2003; Cadorin et al., 2003). OZone is a zone model taking into account the fuel amount and type, openings, and thermal properties of boundaries and calculates the fire evolution. The adopted temperature-time curve for the model is shown in Fig. 4. Based on the compartment fire analysis, it takes 22 min (5 timesteps) for the fire to reach the maximum temperature. The fire is then in a fully-developed phase for 31 timesteps, followed by the cooling phase.

The structure cell is assumed to contribute to fire spread by radiating energy and generating firebrands only during the fully-developed phase. Due to its floor area, a typical house in a WUI community is usually represented by a few connected structure cells. The raster matrix keeps track of the structure cells that belong to the same house. When the fire in any of these cells reaches a fully developed stage, the rest of the cells belonging to the same house will ignite, unless they have been ignited earlier due to radiation or firebrands from other sources. This mechanism is implemented to mimic the fire spread inside a house.

Vegetative fuels (e.g., piles of needles and leaves) burn faster than structures due to larger aspect ratios, better ventilation, and larger porosity compared to structure fuel (Albini and Reinhardt, 1995; Manzello et al., 2007; Mell et al., 2009; Dietenberg, 2010; Morandini et al., 2013). Therefore, it is assumed that a burning vegetation cell in the model contributes to the spread only by firebrand generation and excludes radiation contribution. Given the limited available data, a vegetation cell burns in 1 timestep after ignition (i.e., 5 min).

The SWUIFT model follows a step-by-step procedure in each timestep of the simulation:

1) Ignitions are input to the model and can be added at any timestep. These known ignitions usually include initial ignitions at time zero where the wildfire line approaches the community or are caused by firebrands received inside the community ahead of the fire.
2) If a structure cell (which is part of a particular house) reaches the fully-developed phase of the fire, the rest of the house cells (that are not ignited by radiation or firebrands) will ignite.
3) Contributions of burning cells are calculated at each timestep. Burning vegetation cells generate firebrands and structure cells with fully-developed fire generate both radiative heat and firebrands.
4) The accumulated energy in unignited structure cells, received from the burning structure cells, is calculated and, if the specified threshold is reached, the cells are ignited.
5) Generated firebrands from burning vegetation cells and structure cells land further down the fire line into the community, following the wind direction, and if enough firebrands are accumulated, unignited cells (vegetation and/or structure) ignite.

Fig. 5 summarizes the procedure listed above. Details of the model are further described in the following subsections.

4.3. Radiation

Thermal radiation is the physical phenomenon by which thermal energy is transferred from one body to another in the form of electromagnetic waves. At any given time, the heat flux at a receiving surface is given by:

$$\dot{q}'' = \phi \varepsilon_e \sigma T_e^4 \quad (1)$$

Where $\dot{q}$" is the radiant heat flux in W/m^2, ϕ is configuration factor, ε_e is the emissivity of the emitting surface, σ is the Stefan-Boltzmann constant (5.67×10^{-8} W/m^{2}K^4), and T_e is the absolute temperature of the emitting surface in K. The emissivity refers to the efficiency of a surface as a radiator, and its value is in the range of 0–1. During fire conditions, most of the hot surfaces, such as smoke or flames, have an emissivity between 0.7 and 1.0 (Buchanan, 2017). The configuration factor, which accounts for cases in which the emitting surface is not directly facing the receiving surface, can be calculated based on Buchanan (2017).

As mentioned earlier, the SWUIFT model assumes that a burning structure cell only emits radiation during the fully developed phase of the fire. Fig. 4 shows the assigned temperature-time evolution of fire to compartments in the study, where the fully developed fire phase starts 5 timesteps after the ignition and lasts for 155 min (31 timesteps). The amount of thermal radiative flux received at a given cell is then determined at every time step, using Eq. (1). Although thermal radiation is independent of the wind speed and direction, the resulting flames are indeed influenced by the wind. In general, flames will be oriented in the direction at which the wind is blowing. To account for the effect of wind on the geometry of the flames, it is assumed that the emitting surface is rectangular in shape and is perpendicular to the direction of the wind. Therefore, only the structures located in front of the emitting surface and including $\pm 90^\circ$ with respect to the wind direction (i.e., half-plane along the wind direction), will receive radiation.

Waterman (1969) observed that a spontaneous ignition of various woods due to a radiant exposure generally occurs when the exposed surface reaches a heat flux of 0.8 cal/cm^2-sec, which is equivalent to approximately 12.5 kW/m^2. Although Waterman observed that ignition occurred after 1 min of exposure to the aforementioned levels of radiation, further research offered more details on the relation of the radiant heat flux and the required time of exposure for spontaneous ignition of wood (Quintiere, 2006). It was shown that the critical ignition fluxes across and along the wood grains are 12.0 kW/m^2 and 9.0 kW/m^2, respectively. The model calculates the aggregated flux at a given surface as the addition of all the individual fluxes generated by all the structure cells that are burning within the fully developed phase of the fire over time. If the flux at any specific point in time exceeds a threshold, ignition will occur. The considered value for the critical ignition flux is 14 kW/m^2 (slightly larger than the reported values in tests which are for bare materials) considering tiling or finishing.

4.4. Fire spotting

Fire spotting is proved to be an important mechanism of fire spread in WUI (Cohen, 2008; Koo et al., 2010; Maranghides et al., 2015; Caton et al., 2017). A firebrand or an ember is a small incandescent particle that has separated from a burning material and transported by wind. If a firebrand lands over a combustible material, it could cause an ignition, spreading the fire to an area distant from the original location. Fire

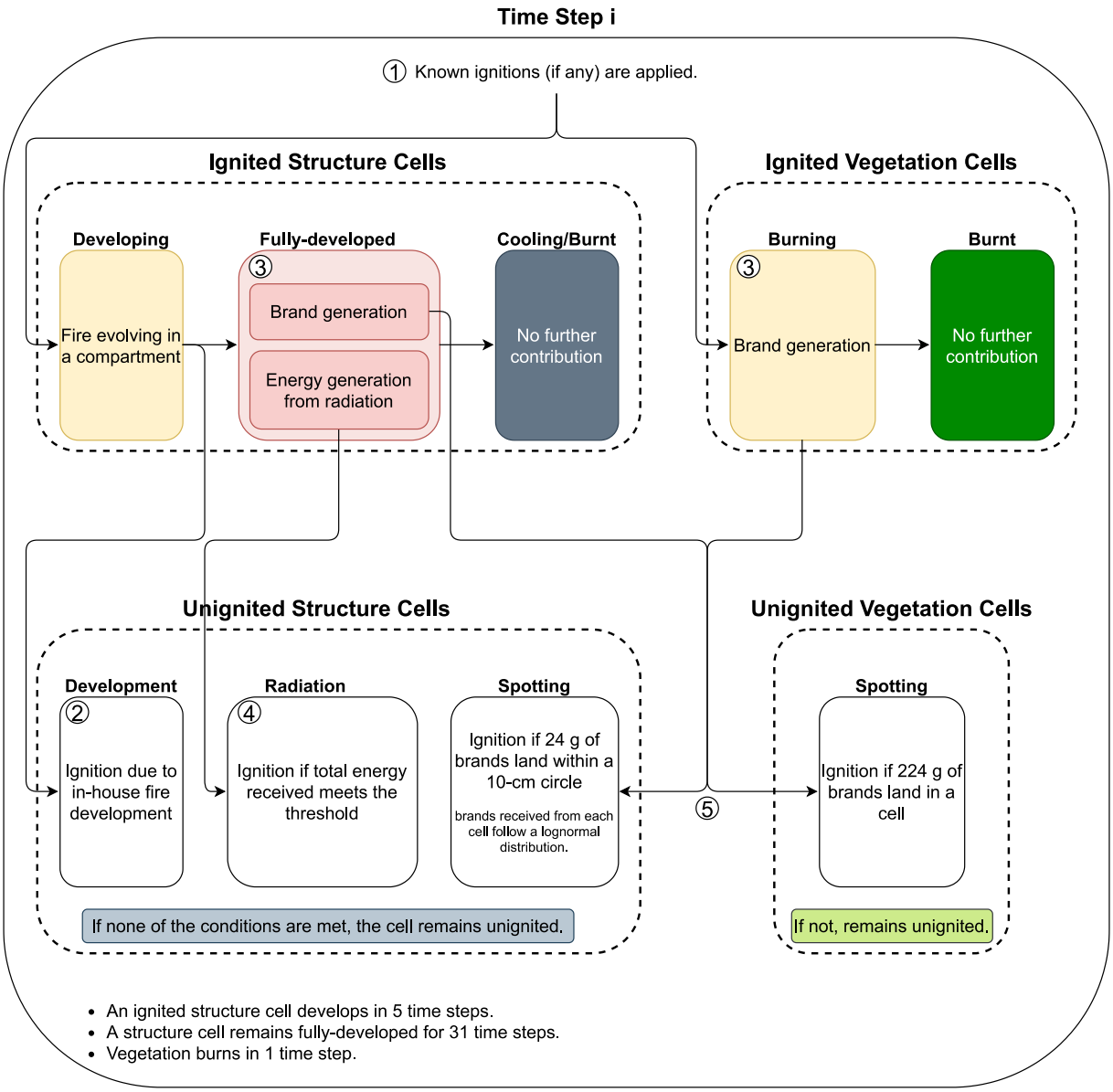

Fig. 5. Flowchart of the SWUIFT model. Number labels indicate the order of operations executed in the code. Color labels will be used to identify different phases when applying the model to two case studies in the following sections.

spotting is a mechanism of fire spread that is difficult to model; therefore, to this date, there is no available definitive physics-based procedure for modeling the three phases of spotting– generation, transport, and ignition – in a holistic approach. The three phases should be properly accounted for in a fire spread model to successfully replicate the occurrence of ignitions during a fire event. For the purpose of this study, a combination of experimental data and probabilistic models is adapted to quantify ignition due to firebrands.

The process of fire spotting starts with particles of burning material detaching from the fuel body. They are then transported by the atmospheric turbulence intensified by the fire. Eventually, the particles will exit the turbulent flow and land on surfaces. The maximum height at which the particles elevate and the characteristics of their trajectory are influenced by the characteristics of the fire weather as well as their shape and density, which in turn are closely related to the specific characteristics of the vegetation or material that is burning. An ignition can occur if one or several incandescent firebrands land over a combustible material. Some firebrands would have been completely consumed through combustion and their temperature would have considerably reduced when they land, lowering or even eliminating the probability of ignition (Caton et al., 2017; Hakes et al., 2017).

Given the number of involved contributing factors and the substantial variation at different stages of spotting, many studies have been conducted focusing on one of the three phases. These studies generally include data collection from real incidents or experimental works. Studies have investigated various features of firebrands such as mass, size, type of material which will be discussed in the following sections. In the SWUIFT model, both vegetation and structure cells generate firebrands, and in return, can potentially get ignited by firebrands. The implemented firebrand model in this study is based on the review and analysis of an extensive collection of studies. Considering the involved uncertainty and unknowns, and to avoid the expensive computational cost, the mass of firebrands is used as the key parameter in the model while assuming that the firebrands are identical in shape. The following sections provide details of the simulated procedure for fire spotting.

4.4.1. *Generation of firebrands*

Different experimental studies (in laboratory or field) have been

conducted to investigate firebrand generation from different fuels and their characteristics such as mass, size, projected area, number of particles, etc. Various features affect the characteristics of a firebrand, such as the surrounding airflow, fire intensity, fuel moisture content, and fuel type. Some studies have focused on vegetative fuels (Manzello et al., 2009; El Houssami et al., 2016; Filkov et al., 2017; Bahrani, 2020; Hudson and Blunck, 2020), and some on structural fuels (Yoshioka et al., 2004; Suzuki et al., 2013, 2014; Suzuki and Manzello 2016, 2021). Despite different conditions and high variations in experiment setups, a common finding among these studies is that the majority of generated firebrands are small (<1 g) with heavy right tail distributions in both mass and cross sectional area. This finding is aligned with reports compiled after fire incidents (Foote et al., 2011; Rissel and Ridenour, 2013; Hasemi et al., 2014; Suzuki, 2017). Moreover, the traveling distance of firebrands have been investigated, and no definitive relationship or significant correlation between distance and particle properties (e.g., mass and size) have been found (Suzuki et al., 2012; Hedayati, 2018; Suzuki and Manzello, 2018; Zhou et al., 2019). Putting the results of these studies together, and taking the computational efficiency of the proposed model into account, it is assumed that identical firebrands with a mass of less than 1 g are generated from both structure and vegetation cells. The fuel models are differentiated by the number of firebrands generated in each timestep.

The generation of firebrands by a structure cell is modeled based on the relation proposed by Lee (2009), describing the number of firebrands produced from a single building as a function of the wind speed. The relationship was derived based on the experimental findings of Waterman (1969). Waterman (1969) reported results of an experimental study on firebrand generation by various roof constructions, including full-scale segments of wood shingles, asphalt shingles, roll roofing, cement-asbestos shingles, built-up roofing, and no covering. Firebrand production was studied under the internal pressure of the fire chamber and with additional pressures to simulate more intense fires and/or wind effects. The produced firebrands were trapped by a screen enclosure and dropped into a quenching pool. All firebrands were sorted, dried, and weighed. Lee and Davidson (2010b) proposed Equation (2) for the *total* number of generated firebrands from a structure based on the gathered data from the experiments described above.

$$n_{b_{total}} = \left(306.77e^{(0.1879\ v)}\right) \times A_{roof} \tag{2}$$

where v is the wind speed in m s^{-1} and A_{roof} is the roof area in m^2. The roof area is calculated for the defined stereotype building; however, the wind speed varies over each timestep. A burning structure cell generates a firebrand only during the fully-developed phase of the fire (i.e., firebrand generation is time-dependent based on the discussion provided in Section 4.2). Thus, Equation (3) is used to calculate the number of firebrands from a structure cell in a given timestep, where 31 is the number of timesteps that a structure cell burns as a fully-developed fire.

$$n_{b_{str},i} = \frac{(306.77e^{(0.1879v_i)}) \times A_{roof}}{31} \tag{3}$$

Here, v_i is the wind speed at time step i in m s^{-1}.

A recent numerical study (Wickramasinghe, 2020) conducted a reverse analysis to calculate the number of firebrands generated from a Douglas fir tree by tuning inputs of their model to match the data by the National Institute of Standards and Technology (NIST) (Manzello et al., 2007; Mell et al., 2009). The study uses the Fire Dynamic Simulator (FDS) model to simulate and analyze the fire (McGrattan et al., 2013), and the simulation follows a specific distribution of mass to produce firebrands. It is determined that a tree with circular base of 1.5 m in diameter and a height of 2.6 m generates about 87 g of firebrands. Assuming that a 10 m × 10 m vegetation cell is fully covered with vegetation, Equation (4) provides $n_{b_{veg}}$, the number of firebrands generated from a vegetation cell.

$$n_{b_{veg}} = \frac{87}{m_b} \times \frac{10^2}{0.75^2\pi} = \frac{4923}{m_b} \tag{4}$$

where m_b is the mass of a firebrand in the model.

4.4.2. Transfer mechanism of firebrands

Himoto and Tanaka (2005) proposed a probabilistic approach for determining the landing distribution of firebrands. Simulations of firebrands, scattered in a turbulent boundary layer, showed that the travel distances of firebrands in the downwind and the sidewind directions could be described by a lognormal and a normal distribution, respectively (Himoto and Tanaka, 2005). In this approach, the downwind distribution is a function of particle's properties such as width and density as well as surrounding's such as wind speed and heat source dimension, and the sidewind distribution is independent of wind speed and particle's features (Himoto and Tanaka, 2005). In a cellular automata model, inspired by the aforementioned model, Zhao (2011) proposed a simplified ellipse to characterize firebrand travel distance, which was parametrized as a step function of wind speed as a proxy to account for the effect of firebrand spotting. This model is also implemented in another cellular automata model on WUI fire spread (Jiang et al., 2020).

In the present work, the following lognormal and normal distributions are implemented for the dispersion of firebrands generated from a burning cell in downwind (x) and sidewind (y) directions, respectively:

$$p(x) = \frac{1}{x\sigma_x\sqrt{2\pi}} \exp\left\{ -\frac{(lnx - \mu_x)^2}{2\sigma_x^2} \right\} \quad (0 < x < \infty) \tag{5}$$

$$q(y) = \frac{1}{\sqrt{2\pi}\sigma_y} \exp\left\{ -\frac{(y - \mu_y)^2}{2\sigma_y^2} \right\} \quad (0 < y < \infty) \tag{6}$$

In the above equations, $\mu_x = \ln(30 \times v)$ where v is the wind speed in m s^{-1}, $\sigma_x = 0.3$, $\mu_y = 0$, and $\sigma_y = 4.85$. The output values measure the distance from a cell's center point in meters, for example, a generated value of 60 m from Equation (5) for a northerly wind implies that the firebrand lands on the 6th cell south of its origin (each cell is 10 m long).

4.4.3. Ignition mechanism due to firebrands

Multiple experiments have been carried out to study the ignitability of fuel beds of different types and configurations, and the potential of firebrands to cause ignition given their features such as mass, size, burning status (flaming, glowing, smoldering) (Ellis, 2015; Hernandez

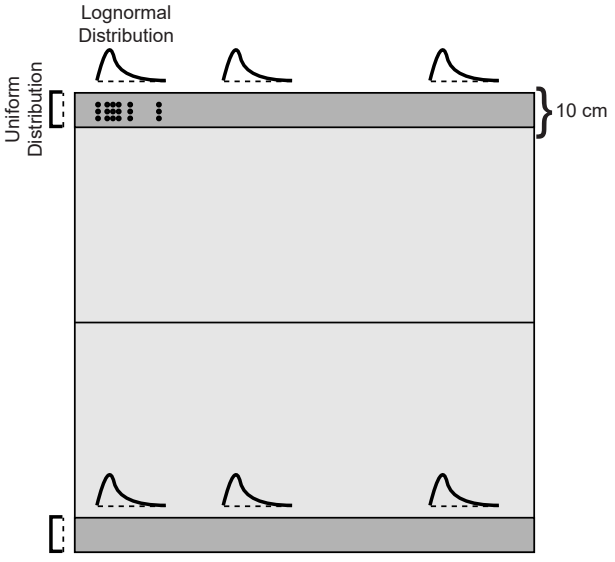

Fig. 6. Schematic of the modeled scatter in firebrands in a structure cell.

et al., 2018; Urban et al., 2019). Some studies compared the potential of ignition by a single firebrand versus a pile of firebrands (Manzello et al., 2006). It has been shown that piles of firebrands have a higher potential to ignite a fuel bed, and the pile mass is a good metric to characterize the pile (Hakes et al., 2019; Tao et al., 2020). The high variation in dimension and mass of individual firebrands make it difficult to characterize a bulk of particles from its constituents, hence the pile mass seems to be more practical for analysis and model application.

Experiments and field studies, specifically for structural components, show that the accumulation of firebrands at corners or interstices increases the chance of ignition (Dowling, 1994; Manzello and Suzuki, 2017; Meerpoel-Pietri et al., 2020). Given that the stereotype house introduced in section 4.2 is designed with a gable roof, it is assumed that accumulated firebrands on two 10 cm stripes on the edges of a cell (i.e., the roof) will be effective to cause ignition. Firebrands received from different cells are scattered on the stripes following probabilistic distributions. The firebrands' landing distributions follow a uniform distribution along the width of the stripes, and a lognormal distribution with the mean of 0.01 and standard deviation of 0.5 along the length of the stripes. Each group of firebrands arriving from a similar source is randomly positioned along the length of the cell. Fig. 6 depicts the stripes and distributions.

Santamaria et al. (2015) investigated the ignition of wooden structures by firebrand accumulation. It is shown that a pile of particles with an initial mass of 60 g deposited on a circular area of 78.53 cm^2 could cause ignition. The mass reduction due to the burning of particles is estimated at 60%. Adapted from this experimental study, here, the ignition condition of a structure cell due to firebrands is determined as the accumulation of 24 g of firebrands landed on a circle with a diameter of 10 cm (area of about 78.53 cm^2) in a given timestep. In other words, a structure cell ignites if there are a sufficient number of firebrands landed close to each other, within a 10-cm circle, on the aforementioned stripes.

To model the ignition due to spotting, typically some values for probability of ignition are assumed for the firebrands (as a function of features such as firebrand size or mass), and ignition of a building is evaluated randomly based on the landed firebrands and the associated probabilities (Himoto and Tanaka, 2008; Himoto et al., 2008; Lee and Davidson, 2010b). The proposed methodology in SWUIFT accounts for the uncertainties associated with ignitions due to firebrands by relating the ignition criterion to the spatial distribution of the particles and their final location on the roof of a building. This way, three points are addressed: (a) the high level of randomness in fire spotting, and (b) the effects of distance and source of the brands since those generated from the same building or vegetation cell are transported and distributed together (See Fig. 6), and (c) the effect of firebrand piles and mass accumulation on ignition.

Suzuki and Manzello (2020) conducted experiments on the effect of accumulation of firebrands on a 1.22 m × 1.22 m shredded hardwood mulch under different wind speeds and moisture contents. The majority of results suggest an ignition time under 300 s (which is equal to the timestep in the SWUIFT model). Also, an upper limit of about 3.5 g of firebrands is required for ignition. A cell in the model can be carpeted by about 64 of such equivalent fuel beds. Hence, a vegetation cell ignites with more than 224 g of firebrands.

5. Application to two case studies

The SWUIFT model is applied to two case studies: (1) the Trails community affected by the 2007 Witch and Guejito fire, and (2) the Fountain Grove community affected by the 2017 Tubbs fire. The two cases are chosen based on the following reasons:

1) The two communities have different layout configurations, such as the size, layout of houses, and vegetation density inside the community.

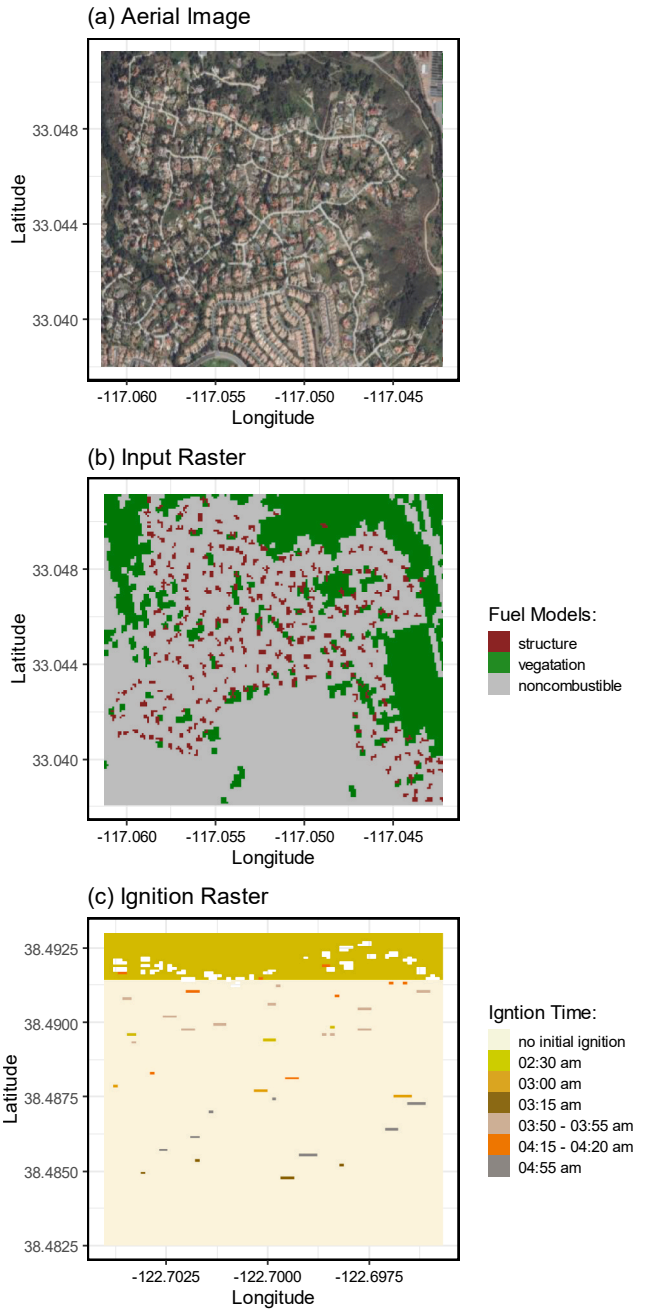

Fig. 7. (a) Aerial image of the Trails community, (b) input raster for the layout and fuel models, (c) input raster for the initial ignitions.

2) The fire behavior in the selected two events was different. In the case of the Trails community, scattered clusters of burned structures were observed. In the second case, the fire line moved quickly over the Fountain Grove community, eventually destroying most of the structures. Furthermore, the effective fire spread duration within the two communities are different.
3) The availability of information to initialize the ignitions and validate the model performance is important. Detailed data, especially for the Trails community, is available.

The two case studies provide the opportunity to evaluate the model for different scenarios. To assess the model's performance, the location of burned structures and the average rate of spread are compared with the observations and measurements from the available references. Although there could be different levels of damage to a structure (i.e.,

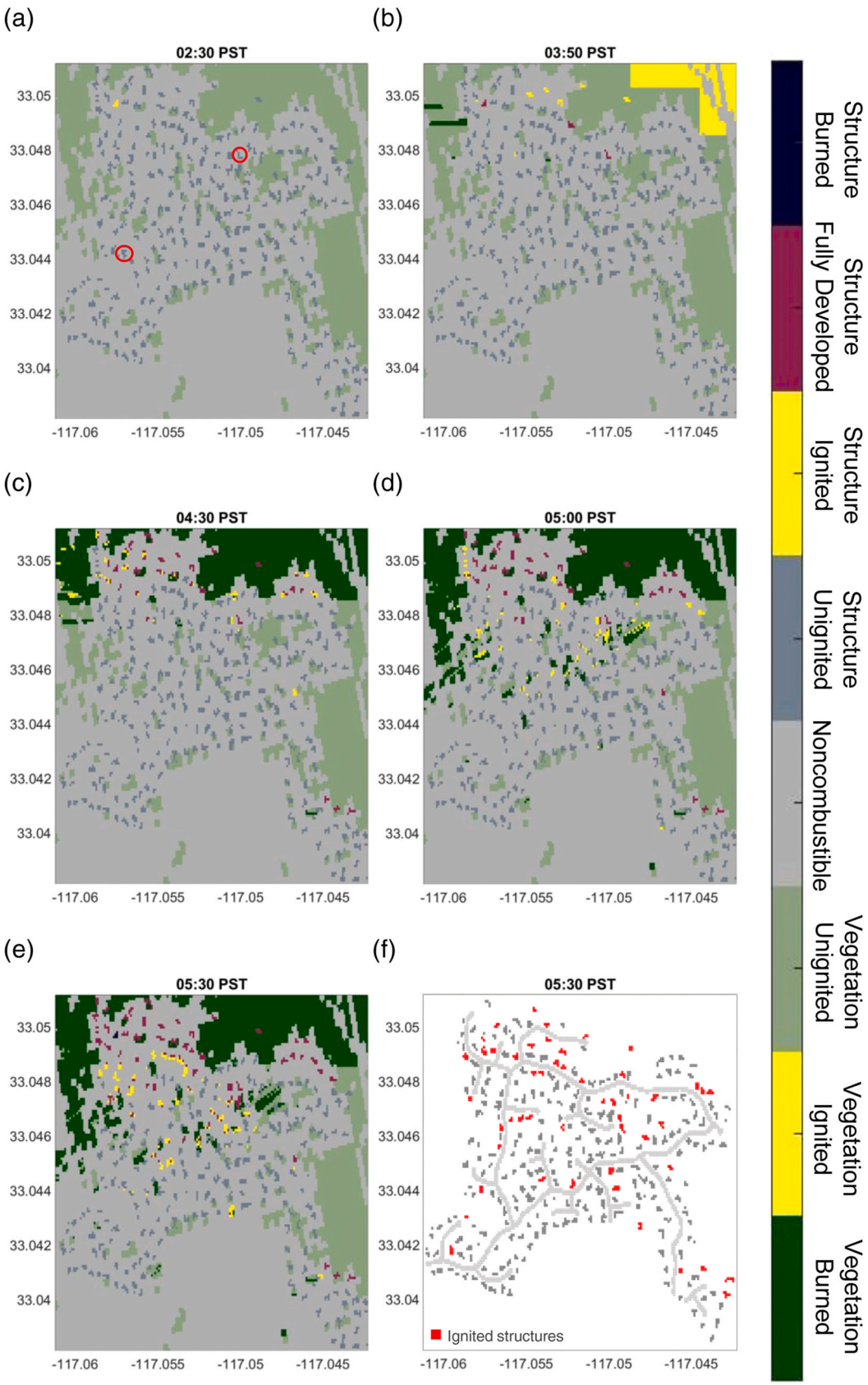

Fig. 8. (a)–(e) Simulated fire spread in the Trails community during the Witch and Guejito fires, (f) structures caught on fire based on observed data.

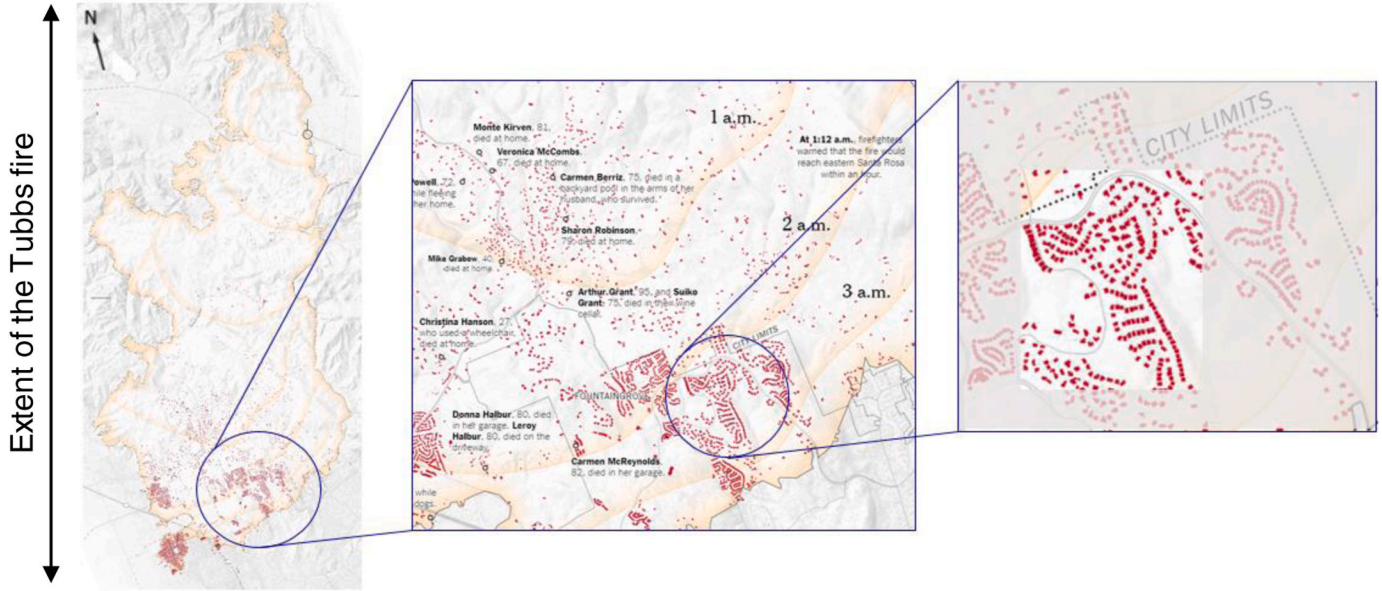

Fig. 9. Left: The extent of Tubbs fire (image from the New York Times, 2017). Right: Highlighted view of the Fountain Grove community.

partially damaged, fully burned), the criterion here is whether or not structures are ignited in the simulation in comparison with the real case, and ideally, if a similar spread rate is observed.

5.1. The trails community

On October 22, 2007, the Trails community in Ranch Bernardo, California, was hit by two wildfires; namely the Guejito fire from the north and, and a few hours later, the Witch fire from the southeast. Although the affected structures were scattered across the community, most of them were located on the northern side of the community which was hit by the Guejito fire. Detailed information about this incident can be found in published reports by NIST (Maranghides and Mell, 2009, 2011; Maranghides et al., 2013).

While it was estimated that the fire line reached the community at around 3:50 a.m. (all reported times are in the local time zone), the first structure ignition inside the community was reported at 2:30 a.m. when the fire was more than 4 km away. Some other houses that were also located close to the northern interface of the community with the wildland were ignited before the arrival of the fire front. Based on the descriptions in the NIST reports, Szasdi Bardales (2019) concluded that a total of 48 structures were ignited inside the community until 5:30 a.m. These ignitions might have been caused by the direct effect of the wildfire or as a result of building-to-building fire propagation. Szasdi Bardales estimated the locations of the structures that were ignited directly due to the wildfire from the wildland. The same cluster of ignitions is implemented as the initial ignition points in the model. Fig. 7 illustrates the layout of the community and the inputs for the model.

The fire scenario is simulated for 3 h starting at 2:30 a.m. Over the course of the simulation, the wind is reported along east and northeast directions, driving the general direction of the fire spread. This information is obtained from the historical data at the Ramona Airport weather station. Fig. 8 demonstrates the simulated fire spread inside the community. The status of structures at 5:30 a.m. is compared with the information extracted from the NIST reports. It is observed that the clusters of burned structures, except for one at the far most southwest, are well-captured. The average FSR based on observed data across the community is estimated as 340 m h^{-1} (Szasdi Bardales, 2019), while Hamada's estimate for FSR was 977 m h^{-1}. Using the simulated results and selecting two structures that are 750 m apart and were ignited at 3:15 a.m. and 5:30 a.m., the calculated FSR from the model is 330 m h^{-1}. The two selected structures are one of the first and last structures ignited over the course of the simulation; the structures are specified by red circles in Fig. 8a.

5.2. The Fountain Grove community

Tubbs fire, the most destructive wildfire in California at the time, was ignited at 9:43 p.m. on October 8, 2017, and in about 4 h, reached the Fountain Grove community, approaching from the north. To the best of the authors' knowledge, there is no reconnaissance report of the Tubb's fire at the time this paper is drafted. However, shortly after the incident, the New York Times (NYT) published an article illustrating the spread of fire at hourly intervals based on data from various sources (Watkins et al., 2017). According to the NYT article, the Tubbs fire reached the Fountain Grove community around 2 a.m. on October 9, 2017 and completely burned the community. Strong north winds were blowing during the time. Fig. 9 depicts the extent of the Tubbs fire in relation to the Fountain Grove community. Based on the available information, the model is applied to the case study starting at 2:00 a.m. and for the duration of 1 h (when the fire line moves out of the community). The layout of the community and the corresponding inputs for the model are presented in Fig. 10.

Fig. 11 illustrates the simulation results. Although not all the structures are ignited during the first hour of simulation, the vegetation is burned to the full extent and the fire front is captured properly. The available information from published articles only estimates the movement of the fire front (the fire front leaves the community around 3:00 a.m.) and not the details about the status of the structures. The estimated FSR based on the observed data is 1780 m h^{-1} (Szasdi Bardales, 2019), while Hamada's estimate was 388 m h^{-1}. Using the simulated results and selecting two structures that are about 600 m apart and were ignited at 2:00 a.m. and 2:30 a.m., the calculated FSR from the model is 1200 m h^{-1}. The two selected structures are specified by red circles in Fig. 11. Based on an article in Los Angeles Times (Krishnakumar et al., 2017), almost all the structures in the community were destroyed, i.e., all of the structures were ignited. If the model runs for a longer duration (until about 4:30 a.m. as shown in Fig. 11e), the rest of buildings will ignite due to fire spread from burning structures. In conclusion, the fire front passes through the community in 1 h, igniting a series of structures and vegetation, which in turn leads to further fire spread to other structures in the hours to follow.

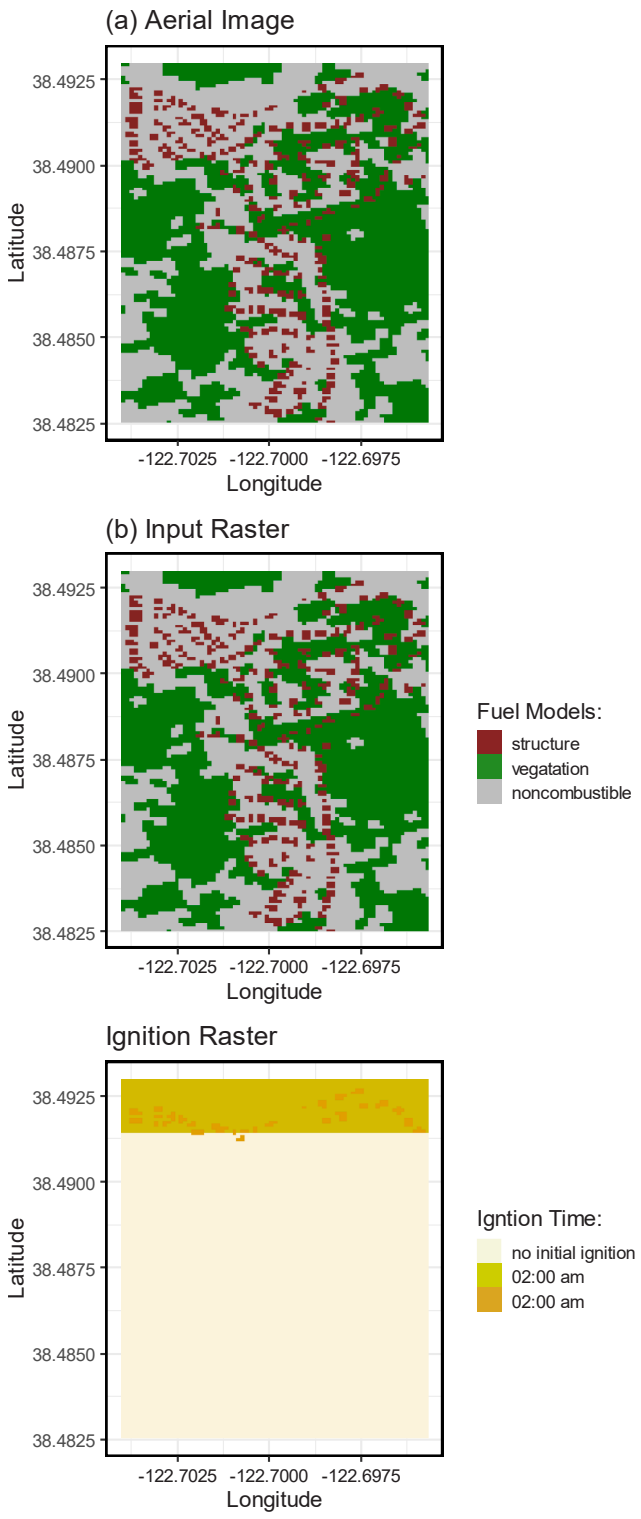

Fig. 10. (a) Aerial image of the Fountain Grove community, (b) input raster for the layout and fuel models, (c) input raster for the initial ignitions.

5.3. Comparison of the two case studies

Further analysis of the model outputs for the two case studies provides insight on the performance of the SWUIFT model. Fig. 12 presents the total number of ignited structures for both case studies and differentiated based on the mode of ignition (spotting, radiation, or known input ignitions). When analyzing the findings, it should be noted that the fire duration and behavior in the two case studies had notable differences.

The effect of fire spotting is apparent in both cases. The model particularly is doing well for the case of the Trails community, where in reality the structural ignitions are scattered over both time and space. In the Fountain Grove community, details cannot be examined due to the lack of data. However, the significant effect of fire spotting is observed as there are ignited structures on the side of the community opposite to and far from the (simulated) fire front in early stages of the simulation. In addition, the spotting takes the fire further ahead of the fire front and radiation causes further expansion of the fire in the proximity of the affected areas.

There are some *idle* intervals (no increase in the number of ignited structures) in the simulations followed by rapid *jumps*. Every simulation begins with an idle interval because it takes five timesteps for the first ignited structure to develop and actively contribute to fire spread, igniting other structures. This justifies the initial idle interval followed by the jumps representing new ignited structures. The same process takes place once new structures are ignited. Also, a quadratic increase in the number of ignited structures, especially those by radiation, is observed over time. This aligns well with the general idea of fire spread which progresses in 2D.

One considerable difference between the two case studies is the defensible actions taken during the event. Defensive actions were taken in the Trails community based on the NIST reports (Maranghides and Mell, 2009, 2011; Maranghides et al., 2013), and they were judged to be effective given the scatter of the burning structures and the limited damage following a good number of ignitions. On the other hand, given the extent of the fire line and the fast spread rate in the Tubbs fire, and the fact that the priority of the first responders is to save lives before saving structures, much could not be done to save structures in the Fountain Grove community, resulting in the whole community burning down. The current version of the model may overestimate the number of burnt structures but future versions will include active firefighting actions to provide guidance for response during wildfire events and study fire spread rates that can be controlled.

6. Discussion

The streamlined model proposed in this study considers the critical mechanisms of WUI fire spread based on the physics of the process and using the available experimental data and empirical models. The effect of direct flame contact is not incorporated in this version of the SWUIFT model. The main reason is that in WUI communities, the separation between structures is considerably larger when compared with urban cities or other non-WUI communities. Yet, it is possible that two (or more) structures are close enough such that one would be at risk of ignition due to direct contact with flames from other structures or nearby vegetations. Future versions of this model will include this mode of fire spread. In general, there are still knowledge gaps on the wildfire phenomenon and corresponding details. Despite the huge efforts, laboratory experiments have not been able to fully replicate the wildfire environment and more data need to be obtained. This is mostly owed to the complexity of these fires, especially on such a large scale and with a high number of variables.

On a typical laptop and using one core of computational power, simulating the cases of Trails and Fountain Grove community fires takes 7 min (Fig. 8e) and 3 min (Fig. 11d), respectively. Computational efficiency is one of the primary objectives of the proposed model. To meet this objective and also due to the lack of available data, some important assumptions are made to simplify the calculations and to generalize the available knowledge. First, the implemented fuel model is independent of the construction type and unique details of structures. The same statement holds true for vegetation. Therefore, the current version of the model differentiates various communities mainly based on their layout. Second, firebrands are assumed to be identical. Although, it is understood that firebrands could have different shapes, using the firebrand

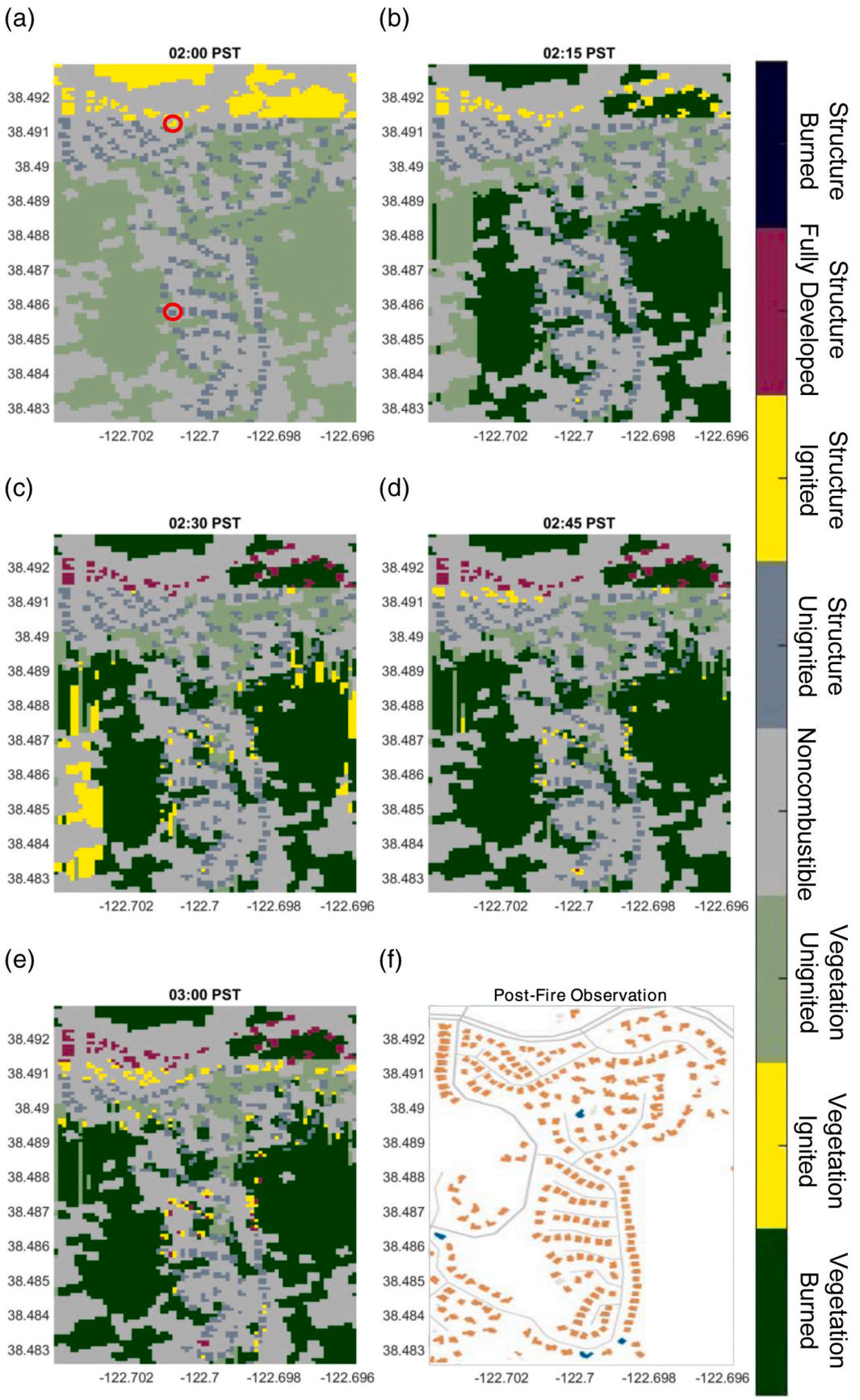

Fig. 11. (a)–(e) Fire spread in the Fountain Grove community during the Tubbs fire, (f) structures caught on fire based on observed data (plot from LA Times, color brown implies destroyed structures and color blue means damaged structures).

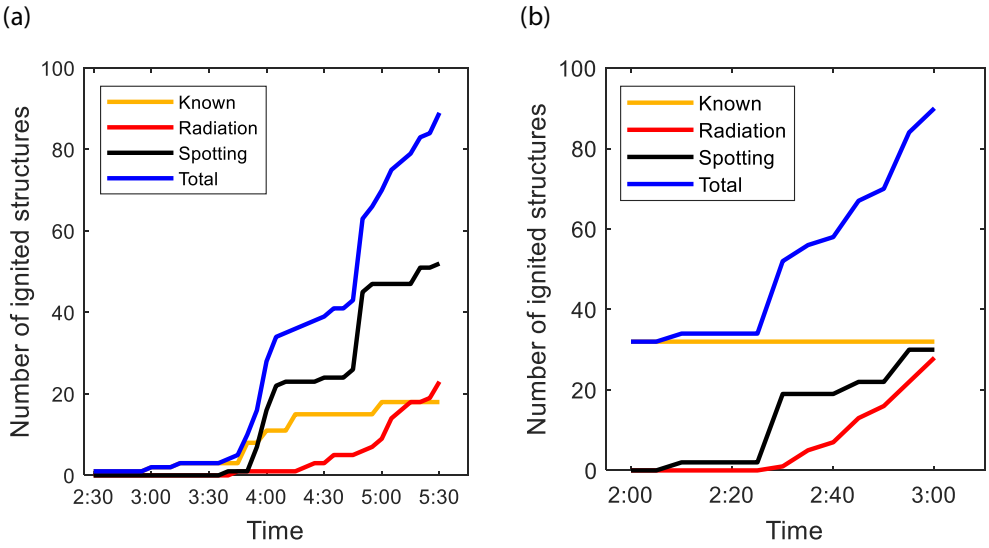

Fig. 12. Number of simulated structure ignitions in the (a) Trails and (b) Fountain Grove communities.

pile mass as the ignition criterion makes the model implementation practical. Third, the effect of spotting is decoupled from the thermal radiative heat flux. Fourth, topography which is known to be a major factor for spread, affecting both radiation and transport of firebrands, is not included in this version of the model.

As discussed in section 5.3, defensible actions before and during an incident play an important role. Suppression actions can be added to the model but there are not many detailed data available for model validation. Moreover, uncertainties in the model parameters can be added in the future.

7. Conclusion

Communities in the wildland-urban interface (WUI) have been exposed to faster spreading wildfires in recent decades and the frequency of destructive WUI fires has been increasing. The available urban fire spread models, which are not inherently designed for WUI fires, cannot capture the fire spread rate (FSR) inside the communities and underestimate the FRS in most cases. This paper proposes a streamlined WUI fire tracing (SWUIFT) model to simulate the spread of WUI fires inside communities. The model relies on the physics of the processes and accounts for Fire spotting and building-to-building spread via radiation, wind velocity and direction, and compartment fire development inside buildings. The established SWUIFT model differentiates communities by considering their layout and land cover at a high resolution (i.e., 10 m).

The SWUIFT model is validated against two historic WUI fires: the Witch and Guejito fires in 2007 and the Tubbs fire in 2017. The two case studies involve two communities with different sizes and building layouts. Moreover, the wildfire scenarios, initial ignitions, and defensible actions during the incidents are distinctly different in the two cases. Hence, the model performance is evaluated for two different WUI fire scenarios. It is shown that the model captures the behavior of fire spread within the communities with a reasonable prediction of FSR and without significant computational cost. The model is also able to distinguish and record the cause of building ignition due to either radiation or firebrands.

The future work will expand the model to include effects of topography and will add a module on first response and suppression actions by firefighters inside a community. The current version of the model leverages empirical relationships for fire spotting and fuel models. As more information and data on such topics become available, the model will be updated accordingly and more detailed fuel models will be included.

Declaration of competing interest

The authors declare that they have no known competing financial interests or personal relationships that could have appeared to influence the work reported in this paper.

Acknowledgements

Fernando Szasdi Bardales gratefully acknowledge partial support for this research from the Fulbright Foreign Student Program and the U.S. Embassy in Guatemala. Any opinions, findings, and conclusions, or recommendations expressed in this material are those of the authors and do not necessarily reflect the views of the Fulbright Foreign Student Program.

This study was partially funded by the State University of New York (SUNY) Research Seed Grant Program. Any opinions, findings, and conclusions expressed in this paper are those of the authors and do not necessarily represent those of the sponsor.

References

Albini, F.A., Reinhardt, E.D., 1995. Modeling ignition and burning rate of large woody natural fuels. Int. J. Wildland Fire 5 (2), 81–91.

Anderson, H.E., 1981. Aids to Determining Fuel Models for Estimating Fire Behavior, vol. 122. US Department of Agriculture, Forest Service, Intermountain Forest and Range Experiment Station.

Bahrani, B., 2020. *Characterization Of Firebrands Generated From Selected Vegetative Fuels in Wildland Fires* (Doctoral Dissertation. The University of. North Carolina at Charlotte).

Bakhshaii, A., Johnson, E.A., 2019. A review of a new generation of wildfire–atmosphere modeling. Can. J. For. Res. 49 (6), 565–574.

Buchanan, A.H., Abu, A.K., 2017. Structural Design for Fire Safety. John Wiley & Sons.

Cadorin, J.F., Franssen, J.M., 2003. A tool to design steel elements submitted to compartment fires—OZone V2. Part 1: pre-and post-flashover compartment fire model. Fire Saf. J. 38 (5), 395–427.

Cadorin, J.F., Pintea, D., Dotreppe, J.C., Franssen, J.M., 2003. A tool to design steel elements submitted to compartment fires—OZone V2. Part 2: methodology and application. Fire Saf. J. 38 (5), 429–451.

California Department of Forestry and Fire Protection, 2020. Top 20 most destructive California wildfires. Available from: https://www.fire.ca.gov/media/5511/top20_destruction.pdf [accessed January 11, 2021].

Caton, S.E., Hakes, R.S., Gorham, D.J., Zhou, A., Gollner, M.J., 2017. Review of pathways for building fire spread in the wildland urban interface part I: exposure conditions. Fire Technol. 53 (2), 429–473.

Cohen, J., 2008. The Wildland-Urban Interface Fire Problem: A Consequence of the Fire Exclusion Paradigm. Forest History Today, pp. 20–26. Fall: 20-26.

Cruz, M.G., Alexander, M.E., Sullivan, A.L., Gould, J.S., Kilinc, M., 2018. Assessing improvements in models used to operationally predict wildland fire rate of spread. Environ. Model. Software 105, 54–63.

Dietenberger, M.A., 2010. Ignition and flame-growth modelling on realistic building and landscape objects in changing environments. Int. J. Wildland Fire 19 (2), 228–237.
Dowling, V.P., 1994. Ignition of timber bridges in bushfires. Fire Saf. J. 22 (2), 145–168.
El Houssami, M., Mueller, E., Filkov, A., Thomas, J.C., Skowronski, N., Gallagher, M.R., Clark, K., Kremens, R., Simeoni, A., 2016. Experimental procedures characterising firebrand generation in wildland fires. Fire Technol. 52 (3), 731–751.
Ellis, P.F.M., 2015. The likelihood of ignition of dry-eucalypt forest litter by firebrands. Int. J. Wildland Fire 24 (2), 225–235.
Filkov, A., Prohanov, S., Mueller, E., Kasymov, D., Martynov, P., El Houssami, M., Thomas, J., Skowronski, N., Butler, B., Gallagher, M., Clark, K., 2017. Investigation of firebrand production during prescribed fires conducted in a pine forest. Proc. Combust. Inst. 36 (2), 3263–3270.
Foote, E.I., Liu, J., Manzello, S.L., 2011. February. Characterizing firebrand exposure during wildland urban interface fires. In: Proceedings of Fire and Materials 2011 Conference. Interscience Communications, London, pp. 479–492.
GISGeography, 2021. How to download free Sentinel satellite data. January 03; Available from. https://gisgeography.com/how-to-download-sentinel-satellite-data/ [accessed January 2021].
Hakes, R.S., Caton, S.E., Gorham, D.J., Gollner, M.J., 2017. A review of pathways for building fire spread in the wildland urban interface part II: response of components and systems and mitigation strategies in the United States. Fire Technol. 53 (2), 475–515.
Hakes, R.S., Salehizadeh, H., Weston-Dawkes, M.J., Gollner, M.J., 2019. Thermal characterization of firebrand piles. Fire Saf. J. 104, 34–42.
Hamada, M., 1975. Architectural Fire Resistant Themes. Kenchikugaku Taikei, Shokokusha, Tokyo.
Hasemi, Y., Yasui, N., Itagaki, N., Izumi, J.I., Osaka, T., Kaku, T., Naruse, T., Hagiwara, I., Kagiya, K., Suzuki, J.I., Kato, K., 2014. August. Full-scale fire tests of 3-story wooden school building. In: World Conference on Timber Engineering. Canada, Quebec City.
Hazus: FEMA, 2014. Hazus: MH 2.1 Technical Manual - Earthquake Model. Developed by the Department of Homeland Security, Federal Emergency Management Agency, Mitigation Division, Washington, DC.
Hedayati, F., 2018. Generation and Characterization of Firebrands from Selected Structural Fuels. Doctoral Dissertation. *The University of North Carolina at Charlotte.* Charlotte, NC.
Hernández, N., Fuentes, A., Consalvi, J.L., Elicer-Cortés, J.C., 2018. Spontaneous ignition of wildland fuel by idealized firebrands. Exp. Therm. Fluid Sci. 95, 88–95.
Himoto, K., Tanaka, T., 2005. Transport of disk-shaped firebrands in a turbulent boundary layer. Fire Saf. Sci. 8, 433–444.
Himoto, K., Tanaka, T., 2008. Development and validation of a physics-based urban fire spread model. Fire Saf. J. 43 (7), 477–494.
Himoto, K., Akimoto, Y., Hokugo, A., Tanaka, T., 2008. Risk and behavior of fire spread in a densely-built urban area. Fire Saf. Sci. 9, 267–278.
Hudson, T.R., Blunck, D.L., 2020. Effects of fuel characteristics on ember generation characteristics at branch-scales. Int. J. Wildland Fire 28 (12), 941–950.
Insurance Information Institute, 2020. Facts + Statistics: wildfires. November 25; Available from. https://www.iii.org/fact-statistic/facts-statistics-wildfires [accessed January 11, 2021].
International Code Council, 2018. 2018 – Internation Wildland-Urban Interface Code. Internaional Code Council, United States.
Iwami, T., Ohmiya, Y., Hayashi, Y., Kagiya, K., Takahashi, W., Naruse, T., 2004. Simulation of city fire. Fire Sci. Technol. 23 (2), 132–140.
Jiang, W., Wang, F., Fang, L., Zheng, X., Qiao, X., Li, Z., Meng, Q., 2020. Modelling of wildland-urban interface fire spread with the heterogeneous cellular automata model. Environ. Model. Software 135, 104895.
Koo, E., Pagni, P.J., Weise, D.R., Woycheese, J.P., 2010. Firebrands and spotting ignition in large-scale fires. Int. J. Wildland Fire 19 (7), 818–843.
Krishnakumar, P., Fox, J., Keller, C., 2017, October, 25. In: Here's where More than 7500 Buildings Were Destroyed and Damaged in California's Wine County Fires. The Los Angeles Times. https://www.latimes.com/projects/la-me-northern-california-fires-structures/ [accessed January 2021].
Lee, S., 2009. Modeling Post-earthquake Fire Spread. Doctoral Dissertation. Cornell University, Ithaca, NY.
Lee, S.W., Davidson, R.A., 2010a. Application of a physics-based simulation model to examine post-earthquake fire spread. J. Earthq. Eng. 14 (5), 688–705.
Lee, S.W., Davidson, R.A., 2010b. Physics-based simulation model of post-earthquake fire spread. J. Earthq. Eng. 14 (5), 670–687.
Lee, S., Davidson, R., Ohnishi, N., Scawthorn, C., 2008. Fire following earthquake—reviewing the state-of-the-art of modeling. Earthq. Spectra 24 (4), 933–967.
Li, S., Davidson, R., 2013a. Application of an urban fire simulation model. Earthq. Spectra 29 (4), 1369–1389.
Li, S., Davidson, R.A., 2013b. Parametric study of urban fire spread using an urban fire simulation model with fire department suppression. Fire Saf. J. 61, 217–225.
Mahmoud, H., Chulahwat, A., 2018. Unraveling the complexity of wildland urban interface fires. Sci. Rep. 8 (1), 1–12.
Mahmoud, H., Chulahwat, A., 2020. Assessing Wildland–Urban Interface Fire Risk, vol. 7. Royal Society open science, p. 201183, 8.
Manzello, S.L., Quarles, S., 2015. *Summary Of Workshop on Structure Ignition in Wildland-Urban Interface (WUI) Fires* (No. Special Publication (NIST SP)-1198).
Manzello, S.L., Suzuki, S., 2017. Experimental investigation of wood decking assemblies exposed to firebrand showers. Fire Saf. J. 92, 122–131.
Manzello, S.L., Cleary, T.G., Shields, J.R., Yang, J.C., 2006. Ignition of mulch and grasses by firebrands in wildland–urban interface fires. Int. J. Wildland Fire 15 (3), 427–431.
Manzello, S.L., Maranghides, A., Shields, J.R., Mell, W.E., Hayashi, Y., Nii, D., 2007. Measurement of firebrand production and heat release rate (HRR) from burning Korean pine trees. Fire Saf. Sci. 7, 108-108.
Manzello, S.L., Maranghides, A., Shields, J.R., Mell, W.E., Hayashi, Y., Nii, D., 2009. Mass and size distribution of firebrands generated from burning Korean pine (Pinus koraiensis) trees. *Fire and Materials*. Int. J. 33 (1), 21–31.
Maranghides, A., Mell, W.E., 2009. A Case Study of a Community Affected by the Witch and Guejito Fires. National Institute of Standards and Technology. Building and Fire Research Laboratory.
Maranghides, A., Mell, W., 2011. A case study of a community affected by the Witch and Guejito wildland fires. Fire Technol. 47 (2), 379–420.
Maranghides, A., McNamara, D., Mell, W., Trook, J., Toman, B., 2013. A Case Study of a Community Affected by the Witch and Guejito Fires: Report# 2: Evaluating the Effects of Hazard Mitigation Actions on Structure Ignitions. National Institute of Standards and Technology, US Department of Commerce and US Forest Service, Gaithersburg, MD.
Maranghides, A., McNamara, D., Vihnanek, R., Restaino, J., Leland, C., 2015. *A Case Study Of a Community Affected by the Waldo Fire Event Timeline and Defensive Actions* (No. Technical Note (NIST TN)-1910).
Masoudvaziri, N., Ganguly, P., Mukherjee, S., Sun, K., 2020. Integrated risk-informed decision framework to minimize wildfire-induced power outage risks: a county-level spatiotemporal analysis. In: Proceedings of the 30th European Safety and Reliability Conference and the 15th Probabilistic Safety Assessment and Management Conference. Venice, Italy.
McGrattan, K., McDermott, R., Weinschenk, C., Forney, G., 2013. Fire Dynamics Simulator, Technical Reference Guide, sixth ed. Special Publication (NIST SP), National Institute of Standards and Technology, Gaithersburg, MD. https://doi.org/10.6028/NIST.sp.1018 [online].
Meerpoel-Pietri, K., Tihay-Felicelli, V., Santoni, P.A., 2020. Determination of the critical conditions leading to the ignition of decking slabs by flaming firebrands. Fire Saf. J., 103017
Mell, W., Maranghides, A., McDermott, R., Manzello, S.L., 2009. Numerical simulation and experiments of burning douglas fir trees. Combust. Flame 156 (10), 2023–2041.
Microsoft, 2019, March 04. Microsoft/USBuildingFootprints. Retrieved from. https://github.com/Microsoft/USBuildingFootprints.
Morandini, F., Perez-Ramirez, Y., Tihay, V., Santoni, P.A., Barboni, T., 2013. Radiant, convective and heat release characterization of vegetation fire. Int. J. Therm. Sci. 70, 83–91.
NFPA, 2021. Firewise USA residents reducing wildfire risk. Available from. https://www.nfpa.org/Public-Education/Fire-causes-and-risks/Wildfire/Firewise-USA [accessed January 2021].
Nüssle, T.A., Kleiner, A., Brenner, M., 2004. June. Approaching urban disaster reality: the resQ firesimulator. In: Robot Soccer World Cup. Springer, Berlin, Heidelberg, pp. 474–482.
Otake, H., Huang, H., Ooka, Y., Kato, S., Hayashi, Y., 2003. Simulation of flames and thermal plume in urban fire under windy condition. In: Proceedings, 17th Japan Society of Fluid Mechanics Symposium, 2-2.
Quintiere, J.G., 2006. Fundamentals of Fire Phenomena.
Reeves, M.C., Ryan, K.C., Rollins, M.G., Thompson, T.G., 2009. Spatial fuel data products of the LANDFIRE project. Int. J. Wildland Fire 18 (3), 250–267.
Rissel, S., Ridenour, K., 2013. Ember production during the bastrop complex fire. Fire management today 72 (4), 7–13.
Rollins, M.G., 2009. LANDFIRE: a nationally consistent vegetation, wildland fire, and fuel assessment. Int. J. Wildland Fire 18 (3), 235–249.
Santamaria, S., Kempná, K., Thomas, J.C., El Houssami, M., Mueller, E., Kasimov, D., Filkov, A., Gallagher, M.R., Skowronski, N., Hadden, R., Simeoni, A., 2015. Investigation of structural wood ignition by firebrand accumulation. In: First International Conference on Structures Safety under Fire Blast, pp. 1–13. Glasgow, UK.
Scawthorn, C., 1987. Fire Following Earthquake: Estimates of the Conflagration Risk to Insured Property in Greater Los Angeles and San Francisco. The Council.
Scawthorn, C., 2009. Enhancements in Hazus-MH Fire Following Earthquake Task 3: Updated Ignition Model. SPA Project No. 10010-01-07-01. Prepared for PBS&J and the National Institute of Building Sciences.
Scawthorn, C., Eidinger, J.M., Schiff, A.J., 2005. Fire following earthquake. In: Technical Council on Lifeline Earthquake Engineering Monograph, no. 26. American Society of Civil Engineers Press, Portland, OR, USA (Book News).
Scott, J.H., 2005. Standard fire behavior fuel models: a comprehensive set for use with Rothermel's surface fire spread model. In: Gen. Tech. Report RMRS-GTR-153. USDA Forest Service, Fort Collins, CO.
Stein, S.M., Menakis, J., Carr, M.A., Comas, S.J., Stewart, S.I., Cleveland, H., Bramwell, L., Radeloff, V.C., 2013. Wildfire, wildlands, and people: understanding and preparing for wildfire in the wildland-urban interface-a Forests on the Edge report. In: Gen. Tech. Rep. RMRS-GTR-299, vol. 36. US Department of Agriculture, Forest Service, Rocky Mountain Research Station, Fort Collins, CO, p. 299.
Sullivan, A.L., 2009. Wildland surface fire spread modelling, 1990–2007. 1: physical and quasi-physical models. Int. J. Wildland Fire 18 (4), 349–368.
Suzuki, S., 2017. Study on characteristics of firebrands collected from three different fires. NRIFD technical report 123, 1–9.
Suzuki, S., Manzello, S.L., 2016. Firebrand production from building components fitted with siding treatments. Fire Saf. J. 80, 64–70.
Suzuki, S., Manzello, S.L., 2018. Characteristics of firebrands collected from actual urban fires. Fire Technol. 54 (6), 1533–1546.
Suzuki, S., Manzello, S.L., 2020. Role of accumulation for ignition of fuel beds by firebrands. Applications in Energy and Combustion Science 1, 100002.

Suzuki, S., Manzello, S.L., 2021. Towards understanding the effect of cedar roof covering application on firebrand production in large outdoor fires. J. Clean. Prod. 278, 123243.
Suzuki, S., Manzello, S.L., Lage, M., Laing, G., 2012. Firebrand generation data obtained from a full-scale structure burn. Int. J. Wildland Fire 21 (8), 961–968.
Suzuki, S., Manzello, S.L., Hayashi, Y., 2013. The size and mass distribution of firebrands collected from ignited building components exposed to wind. Proc. Combust. Inst. 34 (2), 2479–2485.
Suzuki, S., Brown, A., Manzello, S.L., Suzuki, J., Hayashi, Y., 2014. Firebrands generated from a full-scale structure burning under well-controlled laboratory conditions. Fire Saf. J. 63, 43–51.
Szasdi Bardales, F., 2019. Understanding Fire Spread in Wildland-Urban Interface Communities. Thesis, University at Buffalo, New York.
Tao, Z., Bathras, B., Kwon, B., Biallas, B., Gollner, M., Yang, R., 2020. Effect of firebrand size and geometry on heating from a smoldering pile under wind. Fire Saf. J. 103031.
Tokyo Fire Department, 1997. Determinations and Measures on the Causes of New Fire Occurrence and Properties of Fire Spreading on an Earthquake with a Vertical Shock (in Japanese). Tokyo, Japan.
Urban, J.L., Song, J., Santamaria, S., Fernandez-Pello, C., 2019. Ignition of a spot smolder in a moist fuel bed by a firebrand. Fire Saf. J. 108, 102833.
USDA and DOI: United States Department of Agriculture and United States Department of the Interior., 2007. Wildland fire management: the national fire plan. Retrieved from Healthy Forests and Rangelands: http://www.forestsandrangelands.gov/ (accessed January 2021). .
USHF, 2006. Healthy Forests Report: FY 2006 Final Accomplishments.
Waterman, T.E., 1969. *Experimental study of Firebrand Generation* (No. IITRI-J6130-FR). IIT RESEARCH INST CHICAGO IL ENGINEERING DIV.
Watkins, D., Griggs, T., Lee, J.C., Park, H., Singhvi, A., Wallace, T., Ward, J., 2017, October, 21. *How California's most destructive wildfire spread, Hour by hour*, the New York times. Retrieved from. https://www.nytimes.com/interactive/2017/10/21/us/california-fire-damage-map.html [accessed January 2021].
The White House, 2016. FACT SHEET: mitigating the risk of wildfires in the wildland-urban interface. Available from. https://obamawhitehouse.archives.gov/the-press-office/2016/05/18/fact-sheet-mitigating-risk-wildfires-wildland-urban-interface [accessed January 2021].
Wickramasinghe, A., Khan, N., Moinuddin, K., 2020. PHYSICS-BASED SIMULATION OF FIREBRAND AND HEAT FLUX ON STRUCTURES IN THE CONTEXT OF AS3959.
Yoshioka, H., Hayashi, Y., Masuda, H., Noguchi, T., 2004. Real-scale fire wind tunnel experiment on generation of firebrands from a house on fire. Fire Sci. Technol. 23 (2), 142–150.
Zhao, S., 2011. Simulation of mass fire-spread in urban densely built areas based on irregular coarse cellular automata. Fire Technol. 47 (3), 721–749.
Zhou, A., Quarles, S.L.W., David, R., 2019. Fire Ember Production from Wildland and Structural Fuels. JFSP PROJECT ID, 15-1-04-4.